WEIGHTS CONVERGENCE AND SPIKES CORRELATION IN AN ADAPTIVE NEURAL NETWORK IMPLEMENTED ON VLSI

A. Daouzli, S. Saïghi, L. Buhry, Y. Bornat and S. Renaud
IMS-Bordeaux Labs, University of Bordeaux 1
351 cours de la Libération, F-33405 Talence Cedex, France

Keywords: Neuromorphic engineering, STDP, Hodgkin-Huxley model, analog VLSI.

Abstract: This paper presents simulations of a conductance-based neural network implemented on a mixed hardware-software simulation system. Synaptic connections follow a bio-realistic STDP rule. Neurons receive correlated input noise patterns, resulting in a weights convergence in a confined range of conductance values. The correlation of the output spike trains depends on the correlation degree of the input patterns.

1 INTRODUCTION

The first neurophysiology experiments on synaptic plasticity were largely inspired by Hebb's postulate (Hebb, 1949). Today, this postulate is often rephrased in the sense that modifications in the synaptic transmission efficacy are driven by correlations in the firing activity of pre- and postsynaptic neurons. Spike-timing-dependent plasticity (STDP) describes the adaptation temporal mechanisms (depression, potentiation, saturation, ...) at the level of individual spikes (Markram et al., 1997; Bi and Poo, 1998; Abbott and Nelson, 2000; Feldman, 2000; Roberts and Bell, 2002; Kepecs et al., 2002). Synapses with that kind of plasticity were found in the cortex (Markram et al., 1997), in hippocampus cells (Magee and Johnston, 1997) and in cultured cells (Bi and Poo, 1998). First studies showed the existence of Long Term Potentiation (LTP) and Long Term Depression (LTD) dependence, as functions of the synaptic weights to the time difference between the pre- and postsynaptic spikes.

More complex models were developed considering phenomenons such as previous spikes effect for the same neuron (Froemke and Dan, 2002), or the effect of synapse location (Rumsey and Abbott, 2003; Froemke et al., 2005). STDP models can also have different rules depending on the synaptic strength (Bi and Poo, 1998; van Rossum et al., 2000). These models are inspired by biophysical features. Concerning functional aspects, STDP is known to enhance the connections strength for synchronized neurons (van Rossum and Turrigiano, 2001; Song and Abbott, 2001) and is supposed to play a role in neural assembly synchronization (Singer and Gray, 1995). Depending on the shape of the STDP model, the network behavior can change, as the ratio between LTP and LTD influences the weights convergence (Song and Abbott, 2001).

Noise is considered as an interesting input in bio-realistic neural networks as it helps modeling the irregularity of real neuronal activity. Simulations showed also the impact of noise inputs on the synaptic strength evolution when driven by STDP. In (Song and Abbott, 2001), synaptic weights convergence is bimodal. STDP is applied on synapses connecting input noise spike patterns to a single spiking neuron. These input spike trains can be cross-correlated and have a Poisson distribution. With a different STDP rule, where the potentiation (LTP) depends on the synaptic strength, synaptic weights convergence is not bimodal but confined in a limited range (van Rossum et al., 2000).

Here we propose to explore, in a small neural network, the effect of correlated input noise patterns (one pattern per neuron) when a STDP rule is applied on synapses. The effect is evaluated on synaptic (between neurons) conductance distribution and on correlation in neurons' spike trains. Every neuron is attacked by an input noise pattern. These noise patterns have different levels of correlation. We use conductance-based model of cortical neurons.

STDP features are usually explored in large scale spiking neural networks, or in only one single spiking neuron. In this work, we use a 6 neurons network with a complex neuron model based on the Hodgkin and Huxley formalism (Hodgkin and Huxley, 1952). Neurons are implemented on analog VLSI circuits, and the whole simulation system is a mixed hardware-software instrumentation tool (see section 2). These

Daouzli A., Saïghi S., Buhry L., Bornat Y. and Renaud S. (2008).
WEIGHTS CONVERGENCE AND SPIKES CORRELATION IN AN ADAPTIVE NEURAL NETWORK IMPLEMENTED ON VLSI.
In *Proceedings of the First International Conference on Bio-inspired Systems and Signal Processing*, pages 286-291
DOI: 10.5220/0001069102860291

same neural chips have already been successfully used to simulate neural networks with STDP (Zou et al., 2006b). The advantage of analog VLSI for neural simulation is the speed of execution, it ensures simulations in a biological real time. Furthermore, hardware environment provides an electronic noise as in biology living cells are in a noisy environment and emulates in a way biological dispersion. In subsection 2.3, we present the STDP model we use and in subsection 2.4 the method for correlating input noise patterns. Then, in section 3, we show how hardware parameters are related to biophysiological values. In section 4, we present the simulation configuration, tools to observe the distribution of synaptic weights and the correlation of spikes, and we show results and analysis of experiments. Finally, we discuss the specifications and the results of these experiments.

2 THE SIMULATION PLATFORM

We used for the simulation a hardware implementation of a conductance-based neuron model following a Hodgkin and Huxley formalism. The implementation is done on analog VLSI circuits; the neural network connectivity is driven by a custom hardware-software system named PAX (Renaud et al., 2007). This system is embedded on a computer through a PCI interface board.

2.1 The Neurons Models

Analog VLSI circuits, model the neurons ionic currents, as described in the Hodgkin and Huxley formalism. An external capacitor connected to the circuits provides a voltage that is equivalent to the membrane potential and ionic currents channels modulate this potential. Four voltage-dependent ionic currents are implemented: $I_{Na^+}, I_{K^+}, I_{LEAK}$ and a modulating slow voltage-dependent potassium current I_M. The modeled neuron is the glutamate excitatory regular spiking neuron (Connors and Gutnick, 1990). Hardware neurons are characterized by their static parameters as time kinetics, potential offsets, conductance values (table 1), and by their functional features as f(I) curves and spike-frequency adaptation (see section 2.2). The neurons model parameter are listed in table 1. m, n, mm in case of activation and h in case of inactivation are state variables (s), describing the state of ionic channels, defined by: $\tau(V_{MEM})\frac{ds(t)}{dt} = s_\infty(V_{MEM}) - s(t)$ with $s_\infty(V_{MEM}) = \frac{1}{1+exp(\pm\frac{V_{MEM}-V_{OFFSET}}{V_{SLOPE}})}$.

The synapses conductance-based model is the kinetic synapse model presented in (Destexhe et al., 1994). It describes the synaptic strength as the duration of postsynaptic receptors opening (AMPA receptors for excitatory synapses). A pulse length represents the conductance increase due to the release of transmitters (Zou et al., 2006a).

Table 1: Ionic channels parameters for the implemented model, relative to a membrane area of $0.00022cm^2$.

Leak	$I_{LEAK} = g_{LEAK}(V_{MEM} - V_{EQUI})$
	$g_{LEAK} = 33nS, V_{EQUI} = -80mV$
Na	$I_{Na} = g_{Na}m^3h(V_{MEM} - V_{EQUI})$
	$g_{Na} = 11\mu S$, $V_{EQUI} = 50mV$ $m : V_{OFFSET} = -37mV$, $V_{SLOPE} = 7.2mV$ $h : V_{OFFSET} = -42mV$, $V_{SLOPE} = -4.6mV$ $\tau(m) = 0.03ms$, $\tau(h) = \begin{cases} 3.00ms \text{ if } V_{MEM}>0 \\ 0.25ms \text{ if } V_{MEM}<0 \end{cases}$
K	$I_K = g_K n^4(V_{MEM} - V_{EQUI})$
	$g_K = 1.1\mu S, V_{EQUI} = -100mV$ $n : V_{OFFSET} = -37mV$, $V_{SLOPE} = 11.38mV$ $\tau(n) = 3ms$
Mod.	$I_M = g_M m(V_{MEM} - V_{EQUI})$
	$g_M = 10nS, V_{EQUI} = -100mV$ $mm : V_{OFFSET} = -35mV$, $V_{SLOPE} = 11.4mV$ $\tau(mm) = \begin{cases} 300ms \text{ if } V_{MEM}<0 \\ 8ms \text{ if } V_{MEM}>0 \end{cases}$

2.2 Neurons Functional Features

In the PAX system, values of stimulation currents are electronic values that can differ from one neuron to the other to trigger a same frequency. This phenomenon is due to the mismatch and variations in the VLSI circuits fabrication process. We use the f(I) curves to benchmark the circuits and tune the simulation parameters. The measured f(I) curves match the software simulations of the corresponding model. Differences exists concerning origin and scale values for the current range of the f(I) curves. Spike-frequency adaptation shape observed on raster-plots is consistent with biological data. These results are detailed in (Lewis et al., 2006).

2.3 The Neural Network Connectivity

The STDP algorithm used is based on (Badoual et al., 2006) biophysical model equation:

$$+(\omega_{ji} - \omega_{LTD})\sum_l Q[t - \tilde{t}_i(t)]\delta(t - t_{j,l})\Big] \qquad (1)$$

where ω_{ji} is the synaptic weight from neuron j (presynaptic) to i (postsynaptic). $t_{i,k}$ and $t_{j,l}$ are respectively the sets of post- and presynaptic spikes times.

P and Q are respectively the amount of LTP (potentiation) and LTD (depression) change and are given by: $P(t) = A_+ exp(-t/\tau_P)$ and $Q(t) = A_- exp(-t/\tau_Q)$. ε_k are functions taking into account spikes history of a neuron and are given by $\varepsilon_j = 1 - exp[-(t-\tilde{t}_j(t))/\tau_{\varepsilon j}]$ and $\varepsilon_i = 1 - exp[-(t-\tilde{t}_i(t))/\tau_{\varepsilon i}]$. ω_{LTP} is the maximal soft bound while ω_{LTD} is the minimal soft bound. $\tilde{t}_j(t)$ is the neuron j last spike time and $\tilde{t}_i(t)$ is the neuron i last spike time.
The STDP equation (1) is based on a precise biophysical model. Parameters for exponential constants are $A_+ = 0.1$ concerning potentiation and $A_- = 0.005$ for depression. Time constants are $\tau_P = 14.8ms$ for potentiation exponential of P and $\tau_Q = 33.8ms$ for depression exponential for Q. The eligibility ε (influence of previous spikes of a same neuron), has an exponential time constant for the presynaptic neuron $\tau_{\varepsilon j} = 28ms$ and for the postsynaptic neuron $\tau_{\varepsilon i} = 88ms$ (Froemke and Dan, 2002). This takes into account features as frequency dependence and spike triplets. The STDP algorithmic implementation and parameters are detailed in (Zou, 2006).

2.4 Correlated Input Noise Patterns

The noise inputs applied to neurons are coded as patterns generated from a Poisson distribution and correlated with a defined degree. The Poisson distribution X is obtained as follows: $X = \{x_1,..x_n\}/x_i = N(0,1).\sqrt{m-1/2}+m$ where N(0,1) is a normal distribution, m the average. X is converted in an absolute time pattern Y: $X = \{x_1,..x_n\} \rightarrow Y = \{y_1,..y_n\}$:

$$Y : y_i = \sum_{j=1}^{i} x_j \qquad (2)$$

Noise input patterns are generated with one event around each Y event. The time-lap between the event Y and the pattern event is given by ε:

$$\varepsilon = N(0,1).(\alpha - 1).\frac{T}{6} \qquad (3)$$

where N(0,1) is a normal distribution, T is the average period and $\alpha \in [0,1]$ is the correlation coefficient.

3 FIXING HARDWARE/BIOLOGY EQUIVALENCES

The stimulation currents applied to neurons are not directly linked to the biophysical values. The possible values are in the range 0 to 4095. We have the same inconvenience with synaptic conductances. In the hardware, the values are coded as integers that can vary from 0 to 255. To find for each VLSI neuron the correspondence with biophysical values, we developed a neuron model using the software NEURON (Hines and Carnevale, 1997) corresponding to the VLSI neuron model. The morphology of the neuron is a cylinder of 1 section, diameter 96 nm and length 73 nm. Having equivalent models, we developed a protocol to define the biophysical equivalent to the digital parameters values used in PAX.

3.1 Determining Synaptic Conductances in the Pax System

We extracted from the measurements on the PAX system a rule for converting a PAX synaptic strength value in a biophysical corresponding conductance value and conversely. We created a two neurons network (figure 1). Neuron A was stimulated by a current I_A that implies oscillations at about 8.5 Hz. Neuron B is stimulated by a current I_B that implies oscillations at about 3 Hz. Then an excitatory synapse ω_{AB} is created connecting A to B with A presynaptic to B. The synaptic strength increases from 0 to 255 for PAX, 0.02 μS for NEURON. For each weight, neurons frequencies f_A and f_B are measured (f_A doesn't change for NEURON and is near constant for PAX with standard deviation equal to 0.4 and mean value 8.7 Hz). Equations ($f(\omega) = a.\omega + b$) of the straight line fitting the experiments points are calculated for both measurements on PAX and on NEURON. The rules ($\omega_{PAX} = a.\omega_{NEURON} + b$; $\omega_{NEURON} = a'.\omega_{PAX} + b'$) give the correspondence between the biological model and the hardware parameter. Results are: $\omega_{NEURON} = (0.0943\omega_{PAX} + 3.0562)/1070.33$ and $\omega_{PAX} = (1070.33\omega_{NEURON} - 3.0499)/0.0943$.

Figure 1: Network of two neurons A and B stimulated by constant currents, respectively I_A and I_B. ω_{AB} is the synaptic strength of the excitatory synapse connecting A to B.

3.2 Determining Stimulation Currents in the Pax System

The aim here is to extract from measurements a correspondence between a PAX stimulation current value and its biophysical equivalent. The principle is to excite a neuron B by a presynaptic neuron A. A is stimulated as in previous section with a static current. The weight of synapse connecting A to B is also constant.

The B stimulation current varies in a range such that: the lowest value doesn't make B oscillating and the highest value synchronizes B to A firing. Data collected for each neuron B's stimulation current I_B are frequency of B f_B and A's frequency f_A (constant). I_A was chosen to have a frequency $f_A = 8.5Hz$. Using PAX this frequency is approximate (for 10 trials: m=8.7, SD=0.4) due to electronic noise. The simulations duration is 30 s. Frequencies are calculated between 2 s and 29 s. The equivalent synaptic weight is calculated using the rule defined in subsection 3.1. The correspondence is not exactly linear between frequency and current, but the rule that we establish provides a good approximation of the biophysical values corresponding to PAX parameters. This process has to be repeated for every neuron because of their intrinsic variability. We obtain for every PAX neuron, a correspondence rule: $I_{PAX} = a.I_{NEURON} + b$ and $I_{NEURON} = a'.I_{PAX} + b'$. For instance, the rule giving the PAX neuron number 2's biophysical current value is: $I_{NEURON} = -0.01625 I_{PAX} + 36.363$.

4 EXPERIMENTS AND RESULTS

4.1 Experiment: STDP Simulation with Correlation

The PAX system, including the VLSI neurons' was used for the experiments. The system is embedded in a computer, through a PCI interface, that computes plasticity algorithms. The computer features are: processor Intel Pentium 4®, dual core, 2.6GHz, cache: 512 Ko, SDRAM: 1Go. The operating system is the Ubuntu® Linux system. We ran a series of simulations with STDP as described in section 2.3 and noise input patterns as described in subsection 2.4. The simulated neural network comprises six excitatory neurons with all-to-all connectivity. All connections follow a STDP rule. ω_{LTP} is fixed in order to have all neurons presenting a non-bursting activity bursts. The experiment will help evaluating the STDP effects in this small excitatory network when correlated noise patterns are stimulating the neurons.

Network and Neurons Features. The neurons are stimulated by constant currents chosen from f(I) curves to maintain the membrane potential under the firing threshold. Each neuron receive additional stimulation: an input noise pattern (rate 5Hz) tuned in order to trigger an oscillating frequency lower than 5Hz (mean value 3Hz). All currents are in the biological range [0.4nA-0.5nA].

Initial synaptic weights are either null or randomized using an uniform law. Corresponding randomized conductances values, using the correspondence rules determined in section 3.1, are in the range [0nS-20nS] which corresponds to numerical values in the range [0-180]. Furthermore, a neuron receives synaptic inputs from all other neurons and projects its output to all synapses of the other neurons. The simulation lasts 360 seconds. When a neuron spikes, all the related synaptic weights are recalculated using the STDP algorithm. For data analysis, each weight change is recorded together with the timing. For each neuron, all the timing of its spikes are also recorded for further analysis.

4.2 Analysis Tools

Weight Histogram. The method used to assess weight convergence is the building of a histogram of weights distribution (see top line of figure 2). For this experiment, the encoded maximum weight value is 180. We divide the weight axis into 36 bins, thus each section corresponds to an interval of 5. The weights distribution is then calculated at the end of the simulation and normalized.

Spike Correlation Histogram. To evaluate the correlation between the neurons output firing patterns, a correlation histogram is defined (see bottom line of figure 2). The method is to divide the time axis into sections, each section corresponding to 10 ms. Spikes occurring in each time section are accumulated. As we have 6 neurons, the maximum count per section is 6 if every neuron spikes in that 10 ms window, except if a neuron spikes 2 times in the same window. We don't consider that exception here. For every possible spikes count (here from 1 to 6), the number of sections having this value is calculated. Both axis are then normalized. This provides a graph showing the spikes distribution relative to a minimal time window. If the spikes of different neurons are well correlated in that time window, distribution tend to 1, whereas distribution will be closer to 0 for uncorrelated activity.

4.3 Results Analysis

As we can see on the bin histogram of figure 2A, the weights after STDP are distributed in a limited range when the correlation of input patterns is weak ($\alpha < 0.5$, α from equation 3). When the input correlation grows, extrema values of the weights appear (e.g. with $\alpha = 0.6$ figure 2C). When the input correlation is maximum ($\alpha = 1$) then the weights distribution

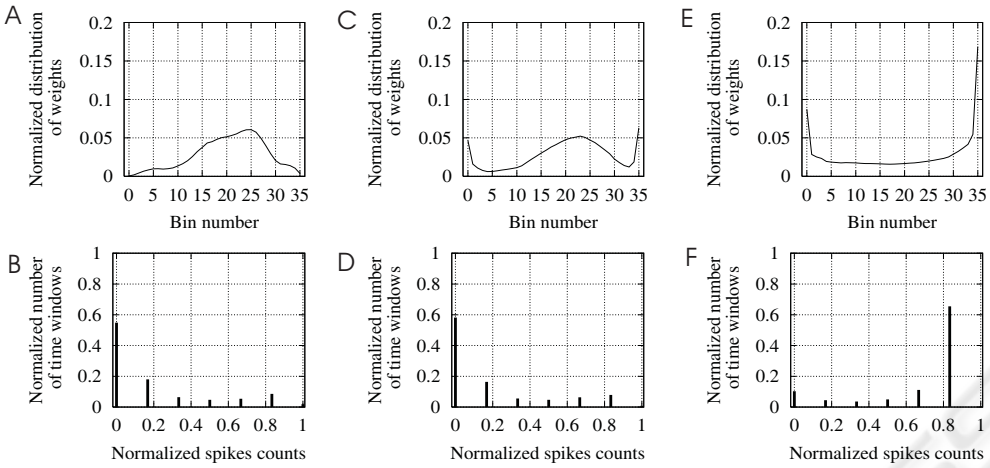

Figure 2: Simulation of input correlation's effect on the synaptic weights convergence and the spikes correlation. Time simulation lasts 360 s with initial weights randomized and a frequency of input noise around 5Hz. *Top line*: Weight histograms for a simulation with input correlation of 0.35 (A), 0.6 (C) and 1 (E). *Bottom line*: Correlation histograms for a simulation with a time window of 10 ms. The input correlations are 0.35 (B), 0.6 (D) and 1 (F).

is bimodal (figure 2E). At the same time, the correlation histogram shows that correlation of output spikes in a window time of 10 ms is weak when correlation input has $\alpha < 0.8$ (figure 2B and D), grows when α is higher. Up to a high correlation when $\alpha = 1$ (figure 2F).

In (van Rossum et al., 2000), where the STDP rule has no soft bound (ω_{LTP} and ω_{LTD}) and where LTP depends on the synaptic strength (ω_{ji}), the weights always converge in a limited range. In (Song et al., 2000), where the soft bound is introduced but with no LTP depending on ω_{ji}, the weights systematically show a bimodal convergence.

Our STDP model was simulated in (Zou and Destexhe, 2007) in single neuron configuration. In that case, all weights converge into a limited range.

The experiments we presented showed that this same STDP rule applied to a 6-excitatory neurons network lead to more complexe figures, mixing bimodal and range limited weights convergence.

5 DISCUSSION AND CONCLUSIONS

Using analog VLSI circuits for computational neuroscience is a performant solution for running simulations at biological real time. The system used can also be interfaced with real biological neurons to create a hybrid neural network (Le Masson et al., 2002). One inconvenient, as seen in section 3, is that the tuning of some parameters depends on the fabrication for parameters. The correspondence rules developed provides an estimation of biophysical values and only in a short range because of non-linearities. However, benchmarks showed us the network patterns were respected by such a simulation tool (Zou et al., 2006a).

In our experiments, we showed that the weights distribution convergence depends on correlation of input noise patterns. This convergence mixes bimodal convergence and range confinement convergence. This phenomenon is not covered by other STDP rules. We also showed that the input correlation degree influences the correlation in neurons spikes. For the next PAX system generation, STDP computation will be embedded in the hardware system. A more important number of neurons will be available with available inhibitory neurons. Experiments will be continued on more complex neural networks.

ACKNOWLEDGEMENTS

This work is supported by the European Community Grant FACETS (IST-2005-15879).

REFERENCES

Abbott, L. F. and Nelson, S. B. (2000). Synaptic plasticity: taming the beast. *Natural Neuroscience*, 3:1178–1183.

Badoual, M., Zou, Q., Davison, A. P., Rudolph, M., Bal, T., Frégnac, Y., and Destexhe, A. (2006). Biophysical and phenomenological models of multiple spike interactions in spike-timing dependent plasticity. *Int. J. Neural Syst.*, 16(2):79–98.

Bi, G. and Poo, M. (1998). Synaptic modifications in cultured hippocampal neurons: dependence on spike tim-

ing, synaptic strength, and postsynaptic cell type. *The Journal of Neuroscience*, 18(24):10464–10472.

Connors, B. and Gutnick, M. (1990). Intrinsic firing patterns of diverse neocortical neurons. *Trends in Neurosciences*, 13:99–104.

Destexhe, A., Mainen, Z., and Sejnowski, T. J. (1994). An efficient method for computing synaptic conductances based on a kinetic model of receptor binding. *Neural Computation*, 6:10–14.

Feldman, D. E. (2000). Timing-based LTP and LTD at vertical inputs to layer II/III pyramidal cells in rat barrel cortex. *Neuron*, 27:45–56.

Froemke, R. C. and Dan, Y. (2002). Spike-timing-dependent plasticity modification induced by natural spike trains. *Nature*, 416:433–438.

Froemke, R. C., Poo, M., and Dan, Y. (2005). Spike-timing-dependent plasticity depends on dendritic location. *Nature*, 434:221–225.

Hebb, D. O. (1949). *The Organization of Behaviour*. John Wiley & Sons.

Hines, M. L. and Carnevale, N. T. (1997). The neuron simulation environment. *Neural Computation*, 9:1179–1209.

Hodgkin, A. L. and Huxley, A. F. (1952). A quantitative description of membrane current and its application to conduction and excitation in nerve. *Journal of Physiology*, 117:500–544.

Kepecs, A., van Rossum, M. C. W., Song, S., and Tegner, J. (2002). Spike timing dependent plasticity: common themes and divergent vistas. *Biological Cybernetics*, 87:446–458.

Le Masson, G., Renaud-Le Masson, S., Debay, D., and Bal, T. (2002). Feedback inhibition controls spike transfer in hybrid thalamic circuits. *Nature*, 417:854–858.

Lewis, N., Bornat, Y., Alvado, L., Lopez, C., Daouzli, A., Levi, T., Tomas, J., Saghi, S., and Renaud, S. (2006). Pax : un outil logiciel / matériel d'investigation pour les neurosciences computationnelles. In *NeuroComp*, pages 171–174.

Magee, J. C. and Johnston, D. (1997). A synaptically controlled, associative signal for hebbian plasticity in hippocampal neurons. *Science*, 275:209–213.

Markram, H., Lubke, J., Frotscher, M., and Sackmann, B. (1997). Regulation of synaptic efficacy by coincidence of postsynaptic APs and EPSPs. *Science*, 275:213–215.

Renaud, S., Tomas, J., Bornat, Y., Daouzli, A., and Saighi, S. (2007). Neuromimetic ICs with analog cores: an alternative for simulating spiking neural networks. In *InternationaI Symposium on Circuits And Systems*, pages 3355–3358. IEEE.

Roberts, P. D. and Bell, C. C. (2002). Spike timing dependent synaptic plasticity in biological systems. *Biological Cybernetics*, 87:392–403.

Rumsey, C. C. and Abbott, L. F. (2003). Equalization of synaptic efficacy by activity- and timing-dependent synaptic plasticity. *The Journal of Neurophysiology*, 91:2273–2280.

Singer, W. and Gray, C. M. (1995). Visual feature integration and the temporal correlation hypothesis. *Annual Review of Neuroscience*, 18:555–586.

Song, S. and Abbott, L. (2001). Cortical development and remapping through spike timing-dependent plasticity. *Neuron*, 32:339–350.

Song, S., Miller, K., and Abbott, L. (2000). Competitive hebbian learning through spike-timing-dependent synaptic plasticity. *Nature Neuroscience*, 3:919–926.

van Rossum, M. C. W., Bi, G.-Q., and Turrigiano., G. (2000). Stable hebbian learning from spike timing-dependent plasticity. *The Journal of Neuroscience*, 20:8812–8821.

van Rossum, M. C. W. and Turrigiano, G. (2001). Correlation based learning from spike timing dependent plasticity. *Neurocomputing*, 38-40:409–415.

Zou, Q. (2006). *Computational models of spike timing dependent plasticity: synapses, neurons and circuits*. PhD thesis, Université Paris VI.

Zou, Q., Bornat, Y., Saïghi, S., Tomas, J., Renaud, S., and Destexhe, A. (2006a). Analog-digital simulations of full-conductance-based networks of spiking neurons with spike timing dependent plasticity. *Network: computation in neural systems*, 17:211–233.

Zou, Q., Bornat, Y., Tomas, J., Renaud, S., and Destexhe, A. (2006b). Real-time simulations of networks of hodgkin-huxley neurons using analog circuits. *Neurocomputing*, 69:1137–1140.

Zou, Q. and Destexhe, A. (2007). Kinetic models of spike-timing dependent plasticity and their functional consequences in detecting correlations. *Biol. Cybern.*, 97(1):81–97.